2018

Effects of Airflow Direction, Air Velocity Profile, and Condensation Pressure on the Performance of Air-Cooled Condensers

William A. Davies
ACRC, University of Illinois, United States of America, daviesi2@illinois.edu

Predrag S. Hrnjak
pega@illinois.edu

Effects of Airflow Direction, Air Velocity Profile, and Condensation Pressure on the Performance of Air-Cooled Condensers

William A. DAVIES III[1], Pega HRNJAK[1,2]*

[1]University of Illinois at Urbana-Champaign,
Department of Science and Engineering,
Urbana, IL, USA
daviesi2@illinois.edu, pega@illinois.edu

[2]Creative Thermal Solutions,
Urbana, IL, USA

* Corresponding Author

ABSTRACT

Experimental results for steam condensation in large, flattened-tube air-cooled condensers are presented. Capacity, void fraction, and steam-side pressure drop and heat transfer coefficient are measured, and visualization is performed simultaneously. Capacity and pressure drop results are discussed here. The condenser tube has an elongated-slot cross-section, with inner dimensions of 214 x 16 mm. The tube is 10.7 m long. Steam mass flux ranges from 6-10 $kgm^{-2}s^{-1}$, average air-side velocities were 1.8 and 2.2 m s^{-1}, and steam condensation pressure ranges from 90-105 kPa. All tests are performed with a horizontal tube and co-current vapor and condensate flow. Three different profiles of cross-flowing air are tested: uniform air flowing upwards, non-uniform air flowing upwards, and uniform air flowing downwards.

Reversing airflow direction from upwards to downwards is found to significantly increase condenser capacity. Capacity is also shown to increase with a non-uniform air-velocity profile in comparison to a uniform air-velocity profile. Both of these performance increases are shown to be the result of matching regions of maximum heat transfer coefficient on the air and steam sides.

Reducing condensation pressure from 105 to 90 kPa is shown to have no effect on capacity, but is shown to increase steam-side pressure drop, due to an increase in steam velocity.

1. INTRODUCTION

Air-cooled condensers (ACCs) provide an alternative to wet-cooled power plants. Closed-cycle wet cooling is the most common cooling technology for newly-constructed United States power plants, but the significant water consumption can put a strain on local water resources (EPRI, 2015). Current ACC designs decrease power-plant efficiency (DoE, 2006) and have higher first cost (EPRI, 2015) than wet-cooling systems. However, ACCs are frequently used when a water source is not readily available or when permitting is difficult. Currently, about 1% of power in the United States is generated using ACCs (Shuster, 2007). This paper investigates methods to improve the efficiency of ACCs, through designs that consider both air- and steam-side effects. In addition, the effect of condensing pressure on condenser performance is evaluated.

Previous studies in both flattened-tube ACCs and in alternative condenser geometries and applications have shown that system performance can be improved by condensate management. Li and Hrnjak (2017a, 2017b) showed that condensation rate can be increased by removing liquid from the condenser, taking advantage of the higher heat transfer coefficient (HTC) of condensing vapor. As one method of removing condensate, Cheng *et al.* (2015) demonstrated numerically that drainage of condensate can be improved by increasing condenser inclination. Kang *et al.* (2017)

confirmed this finding experimentally, and showed that the increased drainage decreases steam-side pressure drop. Davies *et al.* (2018) demonstrated that this improved drainage also increases condenser capacity.

From these results, it is reasonable to conclude that condenser performance can be improved by managing the effects of accumulated condensate in the condenser. This study compares the effect on capacity of two proposed design changes – a non-uniform air velocity profile, and a reversal of the airflow direction.

In addition to altering the condenser design, this paper examines the effect of condenser pressure on condenser capacity and steam-side pressure drop for a power-plant ACC. Condensation pressure is an important system-level parameter. Decreasing condensation pressure improves power-plant performance by increasing the Carnot efficiency, as shown by O'Donovan and Grimes (2014). Only a few previous experimental parametric studies of ACC performance have been performed, and only one in a flattened-tube geometry. Of the previous studies, O'Donovan and Grimes (2015) found that steam-side frictional pressure drop in an ACC bundle increases as inlet vapor velocity increases. However, they also found that momentum recovery also increases, so total pressure drop only increases slightly. They found the correlation of Lockhart and Martinelli (1949) for frictional pressure drop most closely matched their experimental data. In a combined experimental and numerical study of air-steam condensation inside an ACC, Sukhanov *et al.* (2016), found that condensation HTC increased as inlet steam-air velocity increased. However, they found that condensation HTC decreased as subcooling of the condensate decreased. From these results, it is expected that decreasing condenser pressure will increase steam-side pressure drop. The potential effect on capacity is less clear.

2. THEORY

In the flattened-tube ACC design, steam enters in the upper manifold and flows downward in the tubes. Condensate forms along the tube walls, collects in a stratified layer along the tube length, and flows downward under the force of gravity. This co-current downwardly-inclined flow exits the tube at a quality near 20%. The condensate is drained, and the remaining vapor flows upward in counter-current reflux condenser tubes. This paper examines the performance of the downward-flowing co-current condenser tubes, depicted in Figure 1. For these co-current tubes, previous results (Kang et al., 2017) have shown that the flow regime is stratified for nearly the entire tube length. In addition, the depth of the stratified condensate 'river' at the tube bottom increases along the length of the tube. Both filmwise and dropwise condensation have been observed along the tube walls (Davies *et al.*, (2017)). For the transfer of heat, the air side is the dominant resistance for much of the area, the exception being at the air inlet, near the bottom side of the tubes. Air-side HTC is highest at this location, and the steam-side HTC is lowest due to the accumulated condensate layer. This paper investigates designs that diminish the negative impact of this river in order to improve condenser performance.

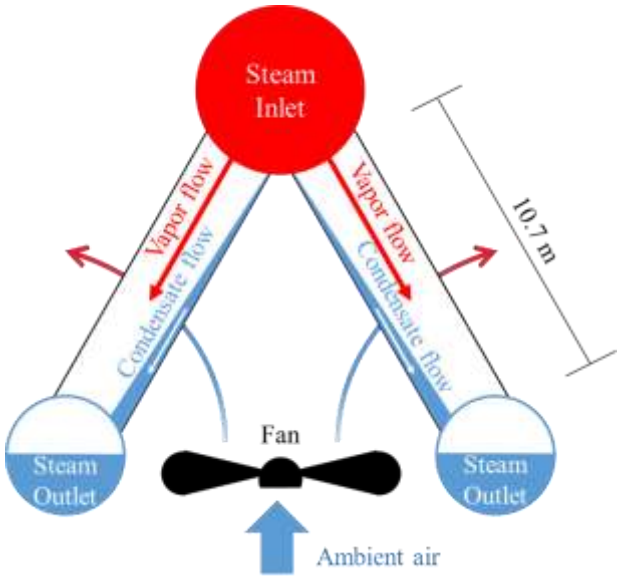

Figure 1: Diagram of co-current downward-flowing tubes in an ACC

3. FACILITY

The experimental facility is the same as that described in Davies *et al.* (2018). The facility schematic is shown in Figure 2 below. The tube can be inclined at the full range of angles from 0 – 90º with steam and condensate flowing co-currently downward. Cooling air is provided by 134 axial fans of 80 mm diameter. The fans are controlled by individual potentiometers to allow for variation of velocity and airflow profile. In this paper, three different airflow profiles are examined: uniform upward flow, non-uniform upward flow, and uniform downward flow.

The tube is a full-length tube equivalent to that in an operating condenser. The length is 10.7 m, consisting of steel walls with aluminum cladding, with aluminum wavy-plate fins along each flat side. The tube has been cut in half lengthwise and a polycarbonate window installed to allow visualization along the entire tube length, as shown in Figure 3.

When running the system at vacuum, ejectors powered by a water loop are used to lower the system pressure. The ejectors are connected at the tube outlet and at the condensate receiver.

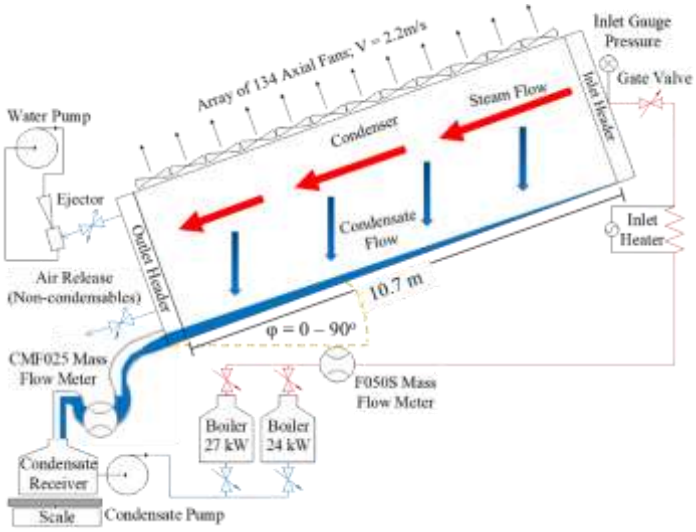

Figure 2: Facility with 10.7 m steam condenser cooled by cross-flowing air

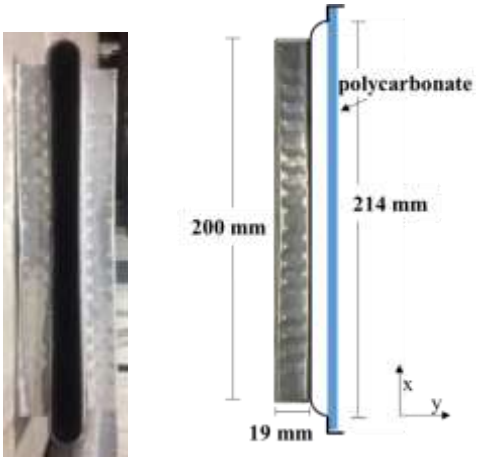

Figure 3: Cross-section views of full tube and tube that has been cut along the centerline. A polycarbonate window allows visualization along the tube length.

Inlet vapor mass flow rate is measured by a Micromotion F050S coriolis mass flow meter, and outlet condensate mass flow rate is measured by a Micromotion CMF025 coriolis mass flow meter. Condensation temperature is measured by T-type thermocouples every 1 m along the tube. Pressure drop is measured in five increments of 2.14 m along the tube length by Rosemount differential pressure sensors. In addition, gauge pressure is measured at the tube inlet and outlet by differential pressure sensors. Air velocity is measured by a hot-wire anemometer that was calibrated in a specially-designed facility. Air velocity has significant local variation, so a total of 645 measurement locations are used to ensure accurate determination of the air flow rate. Air-side inlet and outlet temperatures are measured by T-type thermocouples placed at 0.5 m increments along the tube length.

4. EXPERIMENTAL METHOD

4.1 Experimental Procedure

Steam is provided to the condenser with 0.1 – 0.7 ºC of superheat. At system startup, the fans are switched off until the condenser tube fills with steam. This expels the non-condensable air out of the tube end. Saturation temperature and pressure are monitored at the tube outlet in order to determine air concentration. When these readings indicate 0% concentration of air in the steam, the air release valve is closed and the fans are switched on. System pressure is controlled by increasing or decreasing the boiler power. When running tests at vacuum, the water loops must be switched on occasionally to pump non-condensables out of the system via the ejectors. When all non-condensables

are removed, and system pressure is stable at the desired value, the data are recorded. The valves leading to the ejectors are closed during data acquisition to ensure that no steam is lost from the tube during measurement.

For the current study, test conditions and uncertainties are presented in Table 1.

Table 1: Test conditions

Parameter	Range	Uncert.
Steam mass flux [kg m^{-2} s^{-1}]	7 – 9.5	± 10%
Steam mass flow rate [g s^{-1}]	11 – 13.8	± 0.1%
Condenser capacity [kW]	25.2 – 31	± 3%
Air velocity [m s^{-1}]	1.8, 2.2	± 7%
Vapor inlet pressure [kPa]	90 – 105	± 0.1
Ambient Temperature [°C]	23 – 35	± 0.1
Inlet air temperature difference [°C]	56 – 76	± 0.1
Inclination angle [°]	0	± 0.1

4.2 Data Analysis

Condenser capacity is determined on both the air and steam sides. On the air side, capacity is determined by equation (1.1):

$$Q_a = v_a A_{a,\,face} \rho_a \left(c_{p,ao} T_{ao} - c_{p,ai} T_{ai} \right) + Q_{a,loss} \tag{1.1}$$

On the steam side, capacity is determined by equation (1.2):

$$Q_s = \dot{m}_s \left(i_{si} - i_{so} \right) - Q_{s,loss} \tag{1.2}$$

The values of the heat lost to the atmosphere were determined by independent testing of the system with single-phase hot water. The difference in steam- and air-side capacities were less than 10% for all tests, with an average difference of 3%. To minimize the experimental uncertainty, the capacities were combined into an average capacity using equation (1.3), based on the method of Park and Jacobi (2010):

$$\bar{Q} = \frac{\left(\frac{1}{u_a^{\,2}} \right) Q_a + \left(\frac{1}{u_s^{\,2}} \right) Q_s}{\frac{1}{u_a^{\,2}} + \frac{1}{u_s^{\,2}}} \tag{1.3}$$

Here, u_a and u_s are the air-side and steam-side uncertainties in capacity determination.

Pressure drop is also determined by two methods. The pressure drop of the five individual 2.14 m sections is summed to find pressure drop along the entire tube length, shown by equation (1.4):

$$\Delta P_{total,sum} = \Delta P_1 + \Delta P_2 + \Delta P_3 + \Delta P_4 + \Delta P_5 \tag{1.4}$$

As a second method, the difference between inlet and outlet gauge pressure is also found by equation (1.5):

$$\Delta P_{total,\mathrm{diff}} = P_i - P_o \tag{1.5}$$

The two methods are combined using the method of Park and Jacobi (2010) in order to reduce uncertainty

$$\Delta P_{total} = \frac{\left(\frac{1}{u_{sum}^{\ 2}}\right)\Delta P_{total,sum} + \left(\frac{1}{u_{diff}^{\ 2}}\right)\Delta P_{total,diff}}{\frac{1}{u_{sum}^{\ 2}} + \frac{1}{u_{diff}^{\ 2}}} \tag{1.6}$$

Total pressure drop can also be considered as the sum of three components: gravitational, momentum and frictional pressure drops:

$$\Delta P_{total} = \Delta P_g + \Delta P_m + \Delta P_f \tag{1.7}$$

For a horizontal tube, the gravitational pressure drop is always zero. Momentum pressure drop actually increases the pressure, and is often referred to as momentum pressure recovery. It is the result of the deceleration of the vapor flow, and is calculated by equation (1.8):

$$\Delta P_m = \frac{1}{2}\left[\left(\rho_g v_g^2\right)_{out} - \left(\rho_g v_g^2\right)_{in}\right] \tag{1.8}$$

In the experiment, only condensate exits the tube, so the outlet vapor velocity is zero. The inlet quality and void fraction are approximately equal to one, so the inlet vapor velocity is determined by equation (1.9):

$$v_g = \frac{\overline{Q}}{i_{fg}\rho_g A_{cs}} \tag{1.9}$$

Frictional pressure drop is determined by subtracting the momentum and gravitational pressure drops from the measured total pressure drop.

4.3 Uncertainty

Uncertainties of capacity and pressure drop are determined by the method of Taylor and Kuyatt (1994) on equations (1.3) and (1.6), respectively. Uncertainty of the steam-side capacity is dominated by the measurement of the mass flow rate of condensate. Uncertainty of the air-side capacity is dominated by uncertainty in the outlet air temperature and in the air velocity measurement. Uncertainty of air-side capacity is 7%, of steam-side capacity is 4%, and combined uncertainty of condenser capacity is 1.7%.

Pressure drop uncertainty is determined by the uncertainty of the pressure sensors along with the uncertainty caused by fluctuations in the system pressure. The published sensor uncertainty is 0.2% of the sensor range. The gauge pressure sensors have a range of 0 – 7.5 kPa. The gauges for measuring pressure drop in each 2.14 m section have ranges of 0 - 500 Pa, 0 - 250 Pa, 0 - 250 Pa, 0 -125 Pa, and 0 – 90 Pa for sections 1 – 5 along the condenser, respectively. Significant additional uncertainty was caused by fluctuations in the condenser pressure. The boiling process in the boilers is inherently unsteady, leading to unsteady flow and pressure through the condenser. Therefore, the measured pressure drop experiences significant fluctuation, which leads to an overall uncertainty of total pressure drop of 14%.

5. RESULTS

5.1 Non-Uniform Airflow Profile

Two airflow profiles have been tested: a uniform velocity profile, and a profile with increased velocity near the tube inlet. Both profiles have an average velocity of 1.8 m s^{-1}. The velocity profiles are shown in Figure 4 below.

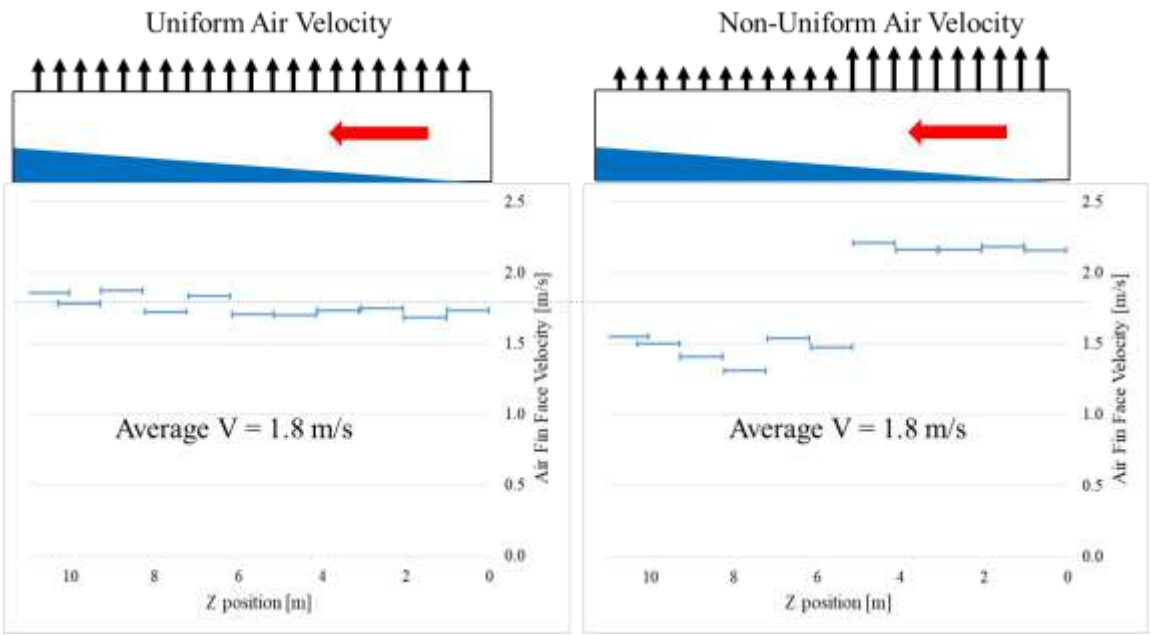

Figure 4: Uniform and non-uniform velocity profiles along the tube length

Results for capacity for both airflow profiles are shown in Figure 5 below. The non-uniform airflow profile has 3.1% higher capacity than the uniform profile. The condenser inlet has the lowest steam-side resistance, due to the lower accumulation of condensate at the bottom of the condenser tube. Therefore, the airflow in this region has more efficacy than the cooling air near the tube outlet. Therefore, it is beneficial to increase airflow at the tube inlet and decrease airflow at the tube outlet.

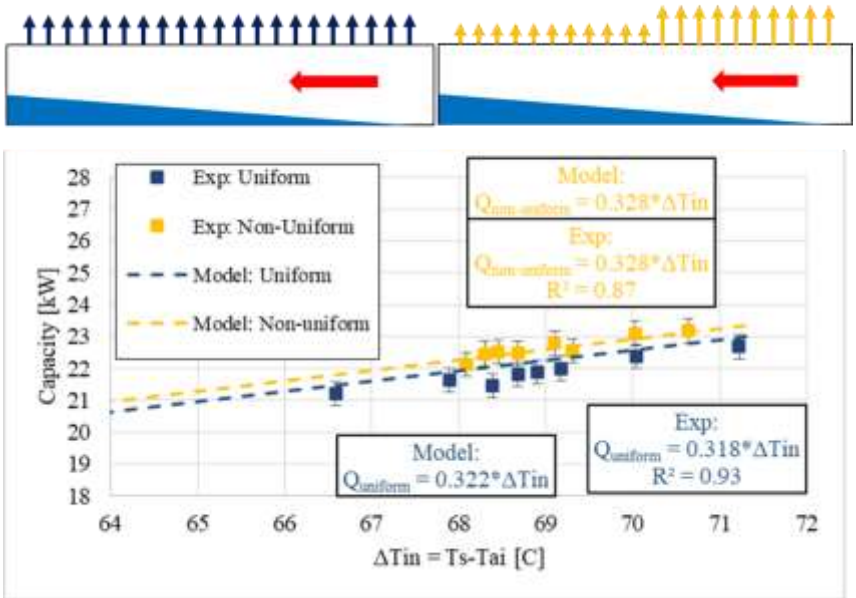

Figure 5: Capacity vs. inlet air - steam temperature difference for two different velocity profiles. Increasing airflow at the condenser inlet increases capacity.

5.2 Reversed Airflow Direction

The effect of airflow direction on condenser capacity is presented in Figure 6 below. The condenser with air flowing downwards has increased capacity in comparison to the condenser with air flowing upwards. At all inlet air – steam temperature differences, the downward-air condenser had 3.5% higher capacity than the upward-air condenser.

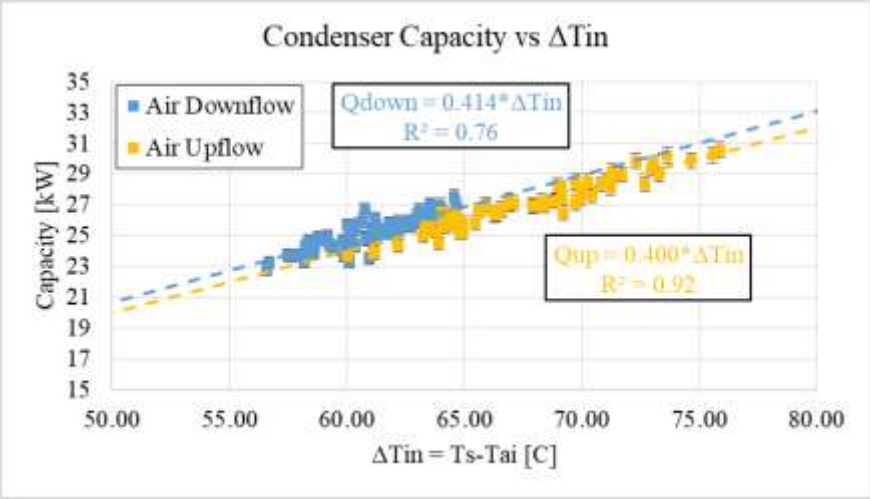

Figure 6: Capacity vs. inlet air - steam temperature difference for air flow upwards and downwards. A condenser with downward air flow has higher capacity than a condenser with upward air flow

The reversal of airflow direction increases capacity by rendering negligible the heat transfer resistance of the condensate layer at the tube bottom. As shown in Figure 7, the condensate layer significantly decreases heat flux at the tube bottom when air is flowing upwards. When air is flowing downwards, the heat flux at the tube bottom is already low, so the decrease due to the added resistance of the condensate is not important to the overall capacity. On the air side, the inlet is the most important region for heat transfer, due to the high ΔT and high HTC. Therefore, it is beneficial to locate this region in a corresponding region of high steam-side HTC. The region of highest steam-side HTC is the tube top (due to the thin film at tube top). Capacity is affected by the sum of the air, steam, and wall resistances, as shown in equation (1.10):

$$Q = AU * \Delta T = A_s \frac{1}{R_a + R_{wall} + R_s}\left(T_s - T_a\right) \tag{1.10}$$

Taken in combination, these two results show the benefit of matching non-uniformities in air and steam-side performance in the condenser.

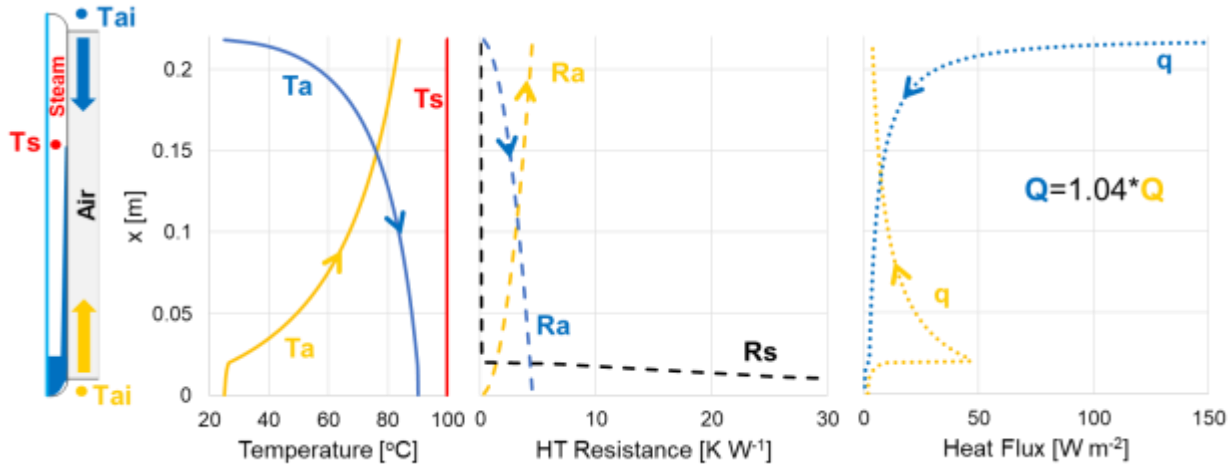

Figure 7: Model for system performance in upward and downward airflow. The resistance of the condensate river has a significant negative effect for the case of upward airflow, but is negligible for the case of downward airflow

5.3 Effect of Condensation Pressure on Capacity and Pressure Drop

The effect of condensation pressure on tube capacity is shown in Figure 8. Condensation pressure is found to have no effect on capacity for both air flowing upwards and downwards. This lack of effect is expected. The two dominant heat transfer resistances – the air side and the stratified condensate layer, are not affected by the steam pressure. The steam pressure is expected to decrease the HTC through the condensate film along the wall. However, this effect is not significant.

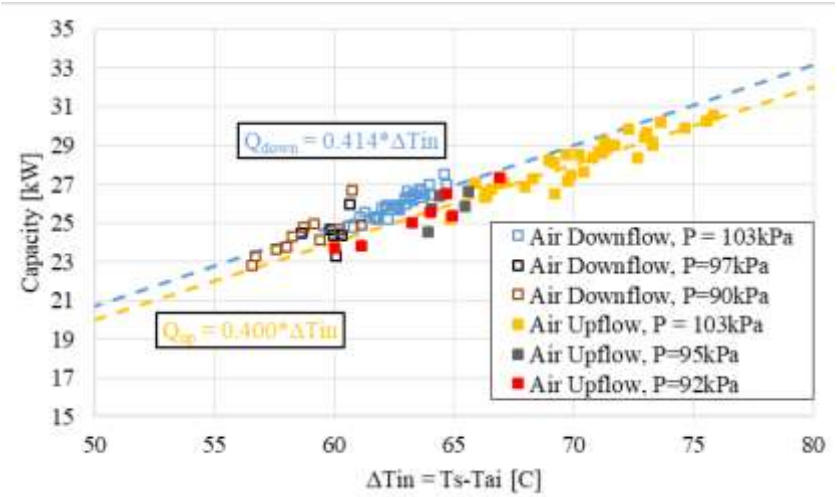

Figure 8: Condenser capacity vs inlet air - steam temperature difference at difference condensation pressures and airflow directions

Figure 9 shows that steam-side pressure drop increases as condensation pressure decreases. This is due to an increase in frictional pressure drop. Frictional pressure drop increases because the vapor velocity increases. Vapor velocity increases due to the decrease in vapor density as pressure decreases.

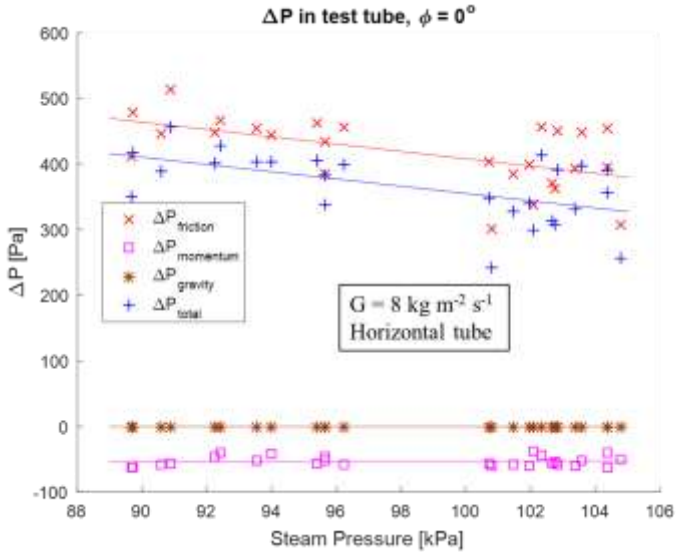

Figure 9: Steam-side pressure drop vs. condensation pressure. Pressure drop increases as condensation pressure decreases

6. CONCLUSIONS

Through experiment, it has been found possible to increase condenser capacity by making modifications to the classic ACC design. These modifications couple knowledge of air- and steam-side condenser performance. Adjusting the air

velocity profile so that more of the airflow is concentrated at the condenser inlet increases capacity. For the tested profile, capacity increases by 3.1% in comparison to a uniform velocity profile. Reversing the airflow direction also increases condenser capacity by 3.5%. This diminishes the negative effect of the high heat transfer resistance of the stratified condensate layer.

In addition to these designs, the effect of condensation pressure on the condenser operation has been tested. Condensation pressure has been found to have no effect on capacity. However, decreasing condensation pressure increases the steam-side pressure drop. Therefore, decreasing condensation pressure decreases the condenser performance. However, this must be balanced with system-level performance, which increases as condensation pressure decreases, due to higher Carnot efficiency.

NOMENCLATURE

A	Area	m^2
c_p	Specific heat at constant pressure	J kg^{-1} K^{-1}
G	Mass flux	kg m^{-2} s^{-1}
i	Specific enthalpy	J kg^{-1}
$\dot{m}$	Mass flow rate	kg s^{-1}
Q	Heat transferred	W
R	Resistance to heat transfer	K m^2 W^{-1}
T	Temperature	^oC
u	Uncertainty	
U	Overall heat transfer coefficient	W m^{-2} K^{-1}
X	Position along wall height	m
x	Vapor quality	
Z	Axial position: z = 0 at tube inlet	m

Subscripts

a	Air
cs	Cross section
f	Fluid
face	Denotes cross-section between fins
G	Gas
i	Inlet
loss	Loss to ambient
o	Outlet
s	Steam

Greek Symbols

α	Void fraction	
ρ	Density	kg m^{-3}

ACKNOWLEDGEMENTS

The authors thankfully acknowledge the support provided by CTS - Creative Thermal Solutions, Inc., the Air Conditioning and Refrigeration Center, the University of Illinois at Urbana-Champaign, and TechnipFMC.

REFERENCES

Cheng, T., Du, X., Yang, L., & Yang, Y. (2015). Co-current Condensation in an Inclined Air-cooled Flat Tube with Fins. *Energy Procedia, 75*, 3154-3161.

Davies, W. A., Kang, Y., Hrnjak, P., & Jacobi, A. M. (2017). *Effect of Inclination on Heat Transfer in Large Flattened-Tube Steam Condensers.* Paper presented at the ASME 2017 International Mechanical Engineering Congress and Exposition.

Davies, W. A., Kang, Y., Hrnjak, P., & Jacobi, A. M. (2018). Method for evaluating the effect of inclination on the performance of large flattened-tube steam condensers with visualization of flow regimes. *Applied Thermal Engineering*.

DoE, U. (2006). Energy demands on water resources: Report to Congress on the interdependency of energy and water. *Washington DC: US Department of Energy, 1*.

EPRI. (2015). *Power Plant Cooling System Overview: Guidance for Researchers and Technology Developers*. Retrieved from Palo Alto, CA:

Kang, Y., Davies III, W. A., Hrnjak, P., & Jacobi, A. M. (2017). Effect of inclination on pressure drop and flow regimes in large flattened-tube steam condensers. *Applied Thermal Engineering*.

Li, J., & Hrnjak, P. (2017a). Improvement of condenser performance by phase separation confirmed experimentally and by modeling. *International journal of refrigeration, 78*, 60-69.

Li, J., & Hrnjak, P. (2017b). Separation in condensers as a way to improve efficiency. *International journal of refrigeration, 79*, 1-9.

Lockart, R., & Martinelli, R. (1949). Proposed correlation of data for isothermal two-phase, two-component flow in pipes. *Chem. Eng. Prog, 45*(1), 39-48.

O'Donovan, A., & Grimes, R. (2014). A theoretical and experimental investigation into the thermodynamic performance of a 50 MW power plant with a novel modular air-cooled condenser. *Applied Thermal Engineering, 71*(1), 119-129.

O'Donovan, A., & Grimes, R. (2015). Pressure drop analysis of steam condensation in air-cooled circular tube bundles. *Applied Thermal Engineering, 87*, 106-116.

Park, Y.-G., Liu, L., & Jacobi, A. M. (2010). Rational approaches for combining redundant, independent measurements to minimize combined experimental uncertainty. *Experimental Thermal and Fluid Science, 34*(6), 720-724.

Shuster, E. (2007). *Estimating freshwater needs to meet future thermoelectric generation requirements*: National Energy Technology Laboratory.

Sukhanov, V., Bezukhov, A., Bogov, I., & Tolmachev, V. (2016). Numerical-Experimental Studies of the Heat Transfer in an Air-Cooled Condenser Model. *Power Technology and Engineering, 50*(3), 318-322.

Taylor, B. N., & Kuyatt, C. E. (1994). NIST technical note 1297. *Guidelines for evaluating and expressing the uncertainty of NIST measurement results*, 24.